Subcontractor Report

Search for Factors Determining the Photodegradation in High-Efficiency a-Si:H-based Solar Cells

**Phase I Annual Technical Progress Report
16 January 1998 — 15 January 1999**

D. Han
*University of North Carolina
Chapel Hill, North Carolina*

NREL

Search for Factors Determining the Photodegradation in High-Efficiency a-Si:H-based Solar Cells

Phase I Annual Technical Progress Report 16 January 1998 — 15 January 1999

D. Han
University of North Carolina
Chapel Hill, North Carolina

NREL

National Renewable Energy Laboratory

NOTICE

Printed on paper containing at least 50% wastepaper, including 20% postconsumer waste

Preface

This Phase I Annual Technical Progress Report covers the work performed by UNC-CH for the period 16 Jan. 1998-15 Jan. 1999 under subcontract No. XAK-8-17619-11.

The following personnel participated in the research program:

Jonathan Baugh, Daxing Han (P.I.), Lei Wu, Guozhen Yue, and Jing Lin.

The samples were obtained from the team members, a-Si group at NREL, G. Ganguly at Solarex, X. M. Deng at U. Toledo, and J. Yang at USSC.

Over the last year, we have benefited from numerous discussions and cooperation with our Condensed Matter colleagues at UNC-CH: Prof. Y. Wu, and Prof. L. E. McNeil. At other institutions we have collaborated with: Dr. G. Ganguly at Solarex, Prof. X.M. Deng at Univ. Toledo, with Prof. G.L. Kong, Institute of Semiconductors, Chinese Academy of Sciences, Prof. S. Nitta, Gifu University Japan, and mostly with Q. Wang and R. S. Crandall et al. at the National Renewable Energy Laboratory (NREL).

Table of Contents

iii

List of Figures

Summary

One objective of this work is to develop improved understanding of carrier collection and open-circuit voltage limitations of a-Si:H-based solar cells. These limitations will be described in terms of transport properties and recombination losses via midgap and tail-state defects. The other objective of this work will verify or disprove the role of hydrogen diffusion as the cause of the metastability. The work will emphasize the investigation of amorphous semiconductor materials and devices known to produce state-of-the-art stabilized device efficiencies, including those deposited by new deposition techniques.

During the first 2 months of Phase I, our laboratory had been innovated. After we moved back, we have successfully upgraded our measurement systems by installing better equipment and LabVIEW software. A grating spectrometer (SPEX TRIAX-180) instead the manual filters has been used in EL spectroscopy (section V shows preliminary results of the spectra); a Keithley 6512 programmable electrometer and a wide-temperature-thermal stage (MMR 78 K- 580 K) have been used in conductivity/photo-conductivity temperature dependence measurements.

In cooperation with Prof. Kong in Beijing, we have characterized of H-bonding and its light-induced changes by using IR and differential IR (DIR) techniques in less-stable and more-stable films. The results will be given in section I. For the less stable film, the IR spectrum is centered at 2040 cm^{-1}; for the more stable samples it is 2000 cm^{-1}. For the less-stable sample, there is a simultaneous decrease near 2040 cm^{-1} and an increase near 1880 cm^{-1}. Light-induced H-bond redistribution could be the origin for such changes. For the more-stable samples, i.e. the hot-wire and the H-diluted GD films, the DIR absorption near 2000 cm^{-1} increases upon light soaking. One possibility is the change of the oscillator strength caused by the change of local charge distribution.

In cooperation with Dr. Wu in our dept., we have characterized H-motion by using NMR. The results will be given in sections II. The dipolar relaxation time T_{1D} of the clustered H is slightly shorter but the T_{1D} of the isolated H is 4 times longer in HW film than that in GD films. We further studied high temperature NMR to clarify the ^{1}H motion. Preliminary results show, in addition to the generic broad and narrow lines in all a-Si:H, a very narrow line (less than 1 kHz wide) is identified as the temperature is raised. This very narrow line is particularly visible and sensitive to temperature in hot-wire a-Si:H.

In cooperation with Prof. S. Nitta in Japan, we have completed a study about the stress of hot-wire a-Si:H. The results will be given in section III. It is clear that the less Si-H bonds the lower compression in the hot-wire films. A photoinduced increase of the compression in the order of 10^{-4} of the initial value was found in all the a-Si:H films including GD and hot-wire a-Si:H. The question is: does the photoinduced volume expansion relate to the SWE? By measuring the optoelectronic properties, we show that these changes are not directly related. In the films deposited at $T_S < 360$ °C, a factor of 4-6 photodegradation of the PC was obtained, but there was no obvious degradation of the PC for the films deposited at $360 < T_S < 440$ °C; whereas, the photoinduced stress were the same. In addition, we found that the surface roughness rather than the bulk defects were responsible for the high PDS sub-band gap absorption signal in the hot-wire a-Si:H films.

By using the transient-null-current method, we have measured the internal electric field profiles $E_i(x)$ near the p/i interface. The results will be given in section IV. we have studied two groups of solar cells: (a) a-Si:H p-i-n solar cells with varied i-layer thicknesses, and (b) a-SiGe:H cells with varied Ge content. From the group (a) samples, our results indicate that for the same quality materials, the thinner the i-layer, the stronger the electric field strength obtained. For the

group (b) a-SiGe:H cells, as the Ge content changes from 55 to 40 %, E_o increases from 9.3×10^4 to 1.2×10^5 V/cm. This is because of a larger optical gap in the a-SiGe:H i-layer with less Ge content.

Further effort will be concentrated on hydrogen motion in relation to SWE by NMR under high temperature and light illumination, and on the material issue in relation to cell performance by EL, PL, and $E_i(x)$ for GD and hot-wire CVD samples.

Our research for Phase I has resulted in the publication of 6 papers (see publications) and the submission of three Quarterly Technical Progress Reports, one Annual Report, and this Annual Technical Progress Report, as well as reports for the team meetings.

Introduction

The central unsolved problem in the study of hydrogenated amorphous silicon (a-Si:H) is the metastability. Although both the material stability and the device performance have been improved step-by-step, the microscopic origin of such metastability is still unclear. Recently, Branz at NREL suggested a H-collision model for the light-induced metastability.[1] This new model explains most of the photo-induced-degradation dynamics including low temperature metastable defects creation. On the other hand, Carlson et al at Solarex has shown that the annealing recovery of the degradation could be accelerated by the application of a strong reverse bias.[2] They suggested that the local motion of protons near silicon dangling bonds results in the acceleration recovery. Both the above models suggested that H motion is crucial for the photodegradation. Can we observe this microscopic local motion? Can we link the H motion with the macroscopic metastability? These are the major issues of our research program. The results are given in sections I, II, and III.

The other issue is to improve understanding of carrier collection and open-circuit voltage limitations of a-Si:H-based solar cells. These limitations will be described in terms of transport properties and recombination losses via midgap and tail-state defects. We carry out internal field profile determinations using the null-current transient measurements for groups of cells with varied (a) Ge content and (b) i-layer thickness. The experimental knowledge of the internal electric profile will then be compared with the results from computer modeling, as well as the cell characteristics such as V_{oc} and J-V. The results are given in section IV. We also continue luminescence measurements and report the progress in Section V.

Technical Progress

I. LIGHT-INDUCED CHANGES OF SI-H BOND ABSORPTION IN A-SI:H FILMS STUDIED BY DIR

I.1 Introduction

Both H-dilution of the conventional glow discharge (GD) and the hot wire CVD deposition technique made devices will exhibit improved stability. These new developments offer a unique opportunity for investigating the detailed involvement of hydrogen in the metastability of a-Si:H by comparing device-quality samples with different degrees of metastability. Hydrogen bonding configurations in a-Si:H have been studied by IR absorption. The sensitivity of the commercial IR spectrometer, including Fourier transform IR, is too low to detect any hydrogen-bonding concentration change less than $10^{21}/cm^3$ in a few µm thick a-Si:H film. Light-induced changes in IR spectra were first reported by Carlson *et. al.* using multiple passages of light through a-Si:H films deposited on prisms [3]. The detected change in IR absorption near 2000 cm^{-1} was about 1-2%. However, the films employed in their experiment were contaminated by oxygen. More recently, R. Dawich et al. [4] reported evidence for participation of atomic hydrogen in the light-induced metastability by FTIR measurement at 6 K on poor-quality a-Si:H. They observed an increasing and then a recovery of the bending band ~ 870 cm^{-1} as well as that of the band at ~ 1720 cm^{-1}, which they attributed to the formation of three center Si-H-Si bonds under illumination. Until recently, there was no reliable technique which has high enough sensitivity to detect the metastable changes of H configurations in device-quality a-Si:H. The invention of the differential infrared absorption (DIR) technique [5] has changed this situation. Using DIR, Kong et al. found [5] that the IR absorption around the wave number 2000 cm^{-1} in a device quality GD a-Si:H increases with light-soaking time; this change is reversible upon annealing. It is our goal

to compare subtle features of H environments between the a-Si:H samples with varied photoinduced metastability.

I.2 Samples and Experimental Conditions

a-Si:H films were deposited on an intrinsic crystalline Si wafer ($\rho > 100$ Ω-cm) by both glow discharge(GD) and hot-wire (HW) CVD at Solarex and the National Renewable Energy Lab (NREL), respectively. The defect density is $\leq 10^{16}$ cm^{-3}. In order to eliminate interference effects, the silicon wafer was single side polished and the a-Si:H film was deposited on the rough side. The sample preparation conditions, thickness, and hydrogen content are listed in Table I. Both infrared (IR) and differential infrared (DIR) absorption spectra were measured by a home-made spectrometer. The measurements were focused on the wave number range from 1800 cm^{-1} to 2300 cm^{-1} where the characteristic peak of the Si-H stretching vibration mode is located. The initial state of the sample was reached by 160°C annealing in a vacuum to remove surface adsorption and metastable defects in the a-Si:H film. Then the measurements were carried out after step-by-step light-soaking. Finally, the sample was annealed at 200 °C in vacuum for one hour to remove the photo-induced defects in the a-Si:H film.

Table I Sample preparation conditions and parameters for DIR studies

Sample ID	Deposition method	Substrate temperature(°C)	Gas	Growth rate (Å/sec)	Film thickness (µm)	H content, C_H (at.%)
SLX, 1	GD-CVD	200	pure silane	4	~5	12-15
SLX, 2	GD-CVD	200	10:1 H-diluted	1	~4	8-10
NREL,3	HW-CVD	410	pure silane	8	~7	~1

The light-induced changes of the Si-H bonds were detected by the specially-designed differential Infrared (DIR) method. In the DIR spectrometer, radiation from an infrared light source is focused on the slit of the monochromator by a reflecting mirror through an IR filter. The monochromatic light passes through the sample and is focused on an IR detector. The sample is mounted in a position where it can rotate about its own axis. The signal collected by the detector is sent to a lock-in amplifier with its reference synchronized to the sample rotation. The sensitivity of DIR is about two orders of magnitude higher than the commercially available IR instruments. This allows us to detect the subtle change of the IR absorption which corresponds to Si-H bond concentration of 10^{18}-10^{19} cm^{-3} in 5 µm thick a-Si:H film. Before light soaking, the lock-in amplifier reads zero since no spatial inhomogeneity modulation is present. Then, half of the film is exposed to light and changed to a metastable state B; the other half stays in the annealed state A. If the light-induced metastable change is accompanied by a change in the IR absorption $\Delta\alpha$, the IR signal will be modulated because of the difference in the IR absorption between the two halves of the a-Si:H film. Consequently, the signal due to $\Delta\alpha$ can be read from the lock-in amplifier. Great care was taken to keep the sample position unchanged after each successive step of illumination.

I.3 Results

I.3.1 IR spectra

The vibration absorption spectra and the normalized curves between 1800 and 2300 cm^{-1} for samples #1, #2, and #3 are shown in Fig. 1(a) and 1(b), respectively. In Fig. 1 (a) the area of the IR spectra is approximately proportional to the total hydrogen content, C_H. Hence, the ratio of hydrogen content is 15 : 7.5 : 2 in the non-diluted, H-diluted, and HW samples. This ratio agrees somewhat with the C_H ratio in Table I that were measured from the area of the IR spectra near 630 cm^{-1}. In Fig. 1 (b), one can see that the peak position and lineshape of the IR spectra are different from each other. Each of the spectra can be resolved into two Gaussion functions as listed in Table II. We call the band near 2000 cm^{-1} the main band and the one near 2100 cm^{-1} the subsidiary band. For the non-H diluted #1 GD film, the main band is centered at 2042 cm^{-1} and the other at 2082 cm^{-1}. The ratio of peak areas of the subsidiary band to the main band is more than 1. For the H-diluted #2 GD film, the main band is centered at 2006 cm^{-1} and the other at 2083 cm^{-1} and the main band dominates (75%) the spectrum. For the #3 HW film, the main band is centered at 2000 cm^{-1} and the other at ~2066 cm^{-1}. The ratio of the subsidiary band to the main band is (43%) less than 1.
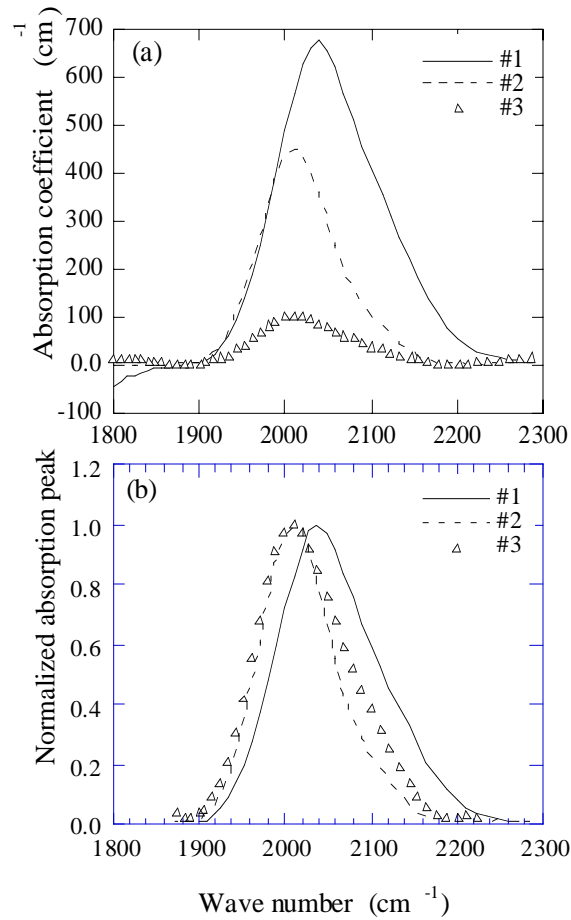
Fig. 1 (a) Absorption of hydrogen bond stretching mode near 2000 cm^{-1} for three a-Si:H samples, and (b) the normalized curves of (a).

5

Table II   Gaussion function deconvolution of the IR spectra

Sample ID	Absorption band	Peak position (cm⁻¹)	Width (cm⁻¹)	Height (cm⁻¹)	Peak area (cm⁻²)	Ratio of the peak area (%)
SLX#1	main band	2042	114	371	53163	47
	subsidiary	2082	202	236	59541	53
SLX#2	main band	2006	75.5	389.5	36838	75
	subsidiary	2083	98.8	98.6	12216	25
NREL#3	main band	2000	78.6	105	10361	57
	subsidiary	2066	106.7	59	7887	43

I.3.2 DIR spectra

The light-induced changes of the hydrogen bond absorption were unable to be detected by conventional IR spectroscopy but were detected by the DIR method. A few curves of the DIR spectra of sample #1 are show in Fig. 2. One can see a decrease of the absorption near 2040 cm⁻¹ where the center of the IR spectrum is as shown in Fig.1(a); meanwhile, an increase centered at 1880 cm⁻¹ is observed. The DIR spectra of sample #2 are shown in Fig. 3. We found an increase of the absorption near 2000 cm⁻¹. This is consistent with the results by Zhao et al.[5] for H-diluted GD a-Si:H films. Figure 4 shows the DIR results for the HW sample #3. One can see that the light-induced DIR signal increases near 2000 cm⁻¹ with behavior similar to that of sample #2 as shown in Fig. 3.
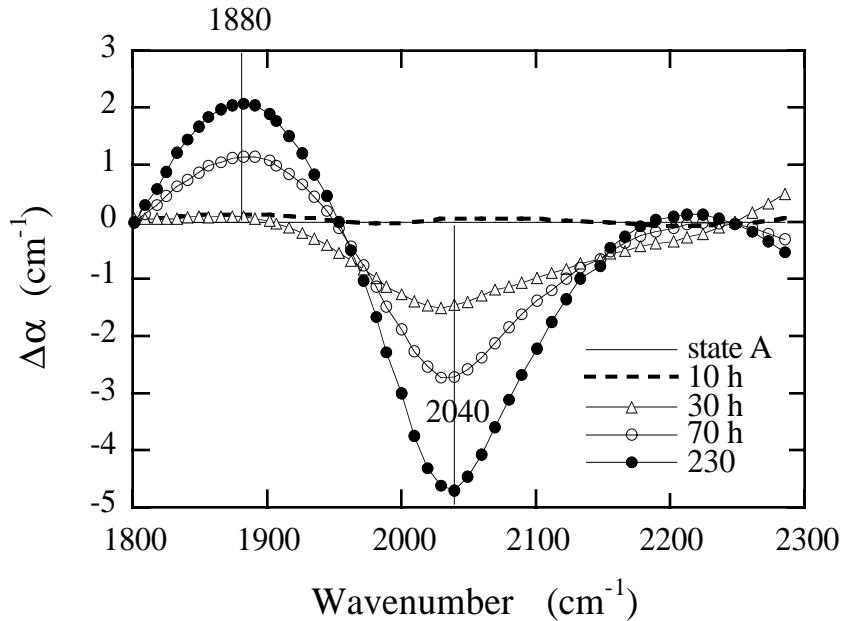
Fig. 2. Light-soaking effect in a non-H-diluted GD a-Si:H film studied by DIR absorption
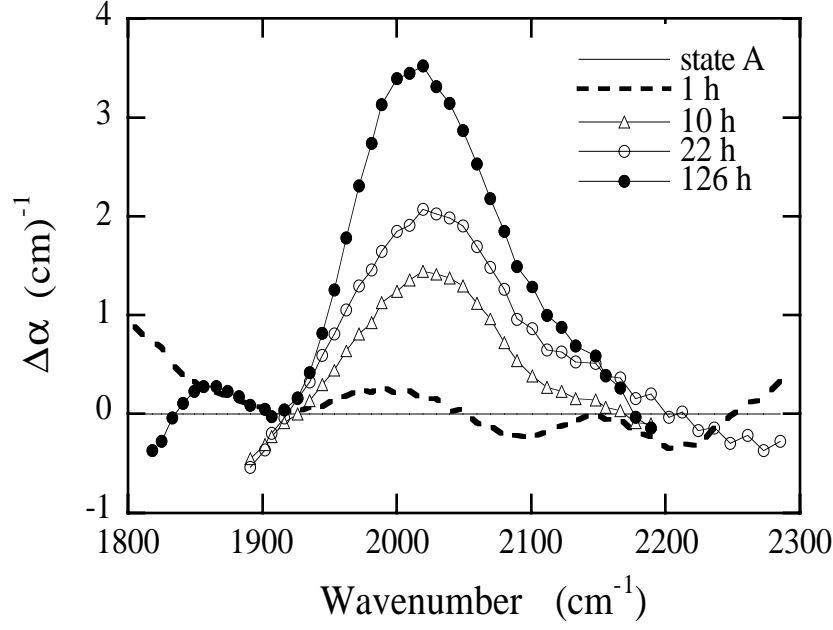
Fig. 3. Light-soaking effect in an H-diluted GD a-Si:H film studied by DIR absorption
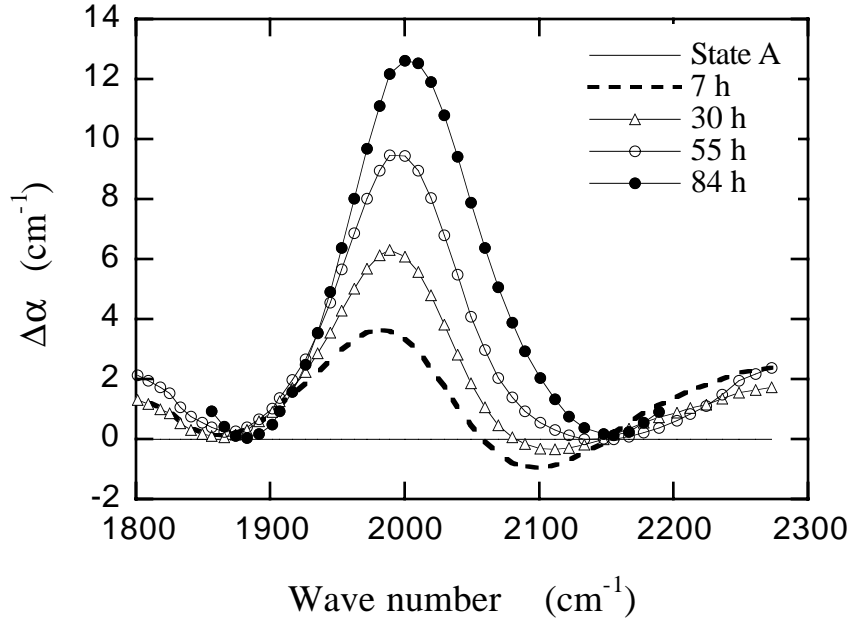
Fig. 4   Light-soaking effect in a HW a-Si:H film studied by DIR absorption

I.4 Summary and Discussion

Three device-quality a-Si:H samples with defect density $\leq 10^{16}$ cm^{-3} were studied. According to photoconductivity measurements, these three samples show varied degrees of photo-induced degradation: higher for non-H-diluted sample #1, and less for H-diluted sample #2 and HW

sample #3. The total H content in these samples varies between 2-15 at.%, i.e. 10^{21}-10^{22} cm^{-3} hydrogen in the network. In order to find the correlation between hydrogen incorporation and the stability, we have measured the IR absorption and its light-induced changes. For sample #1 with 15 at.% H, we found that the IR spectrum is centered at 2040 cm^{-1} instead of 2000 cm^{-1}. This agrees well with the IR data measured by the sample supplier at Solarex. For the more stable samples #2 and #3, the IR spectra are centered near 2000 cm^{-1}. These also agree well with the IR data measured by the sample suppliers at Solarex and NREL. There were no measurable light-induced changes of the IR absorption measured by IR spectrometer for all three samples. However, by using the DIR technique, we have observed the photoinduced changes of the IR absorption. From the experimental results shown in Figs. 2, 3 and 4, we found 0.5-1% photoinduced changes of their IR absorption upon 90 mW/cm^{-2} light-soaking as follows: (a) for the less stable sample #1, there is a simultaneous decrease in the DIR absorption near 2040 cm^{-1} and an increase of absorption near 1880 cm^{-1}. Light-induced H-bond redistribution [1,4] could be the origin for such changes. At this point, we are not sure whether the Si-H trapped in microvoids or the SiH$_2$ species are responsible for the 2040 cm^{-1} peak. The band at 1880 cm^{-1} is likely related to a-Si:H stretch mode at antibond sites [6]. (b) for the more stable samples #2 and #3, the DIR absorption near 2000 cm^{-1} increases upon light soaking. If there was an increase of the density of the Si-H bonds upon light-soaking, it would imply the creation of 10^{19}-10^{20} cm^{-3} of metastable Si-H bonds. The other possibility is the change of the oscillator strength caused by the change of local environments (e.g., local charge distribution) of the Si-H bonds. On the other hand, a photoinduced volume expansion (in the order of 10^{-4}, see section III in this report) was observed that should correlate with the photoinduced DIR increase. However, it can not explain the big (0.5-1%) photoinduced changes of the IR absorption.

II. [1]H MOTION STUDIED BY DIPOLAR ORDER RELAXATION IN A-SI:H FILMS

II.1 Background

It has been found that hot wire a-Si:H is very different from the conventional GD materials, in particular, the H microstructure as detected by nuclear magnetic resonance (NMR) including Multiple-quantum NMR (MQ NMR).[7] We have demonstrated that the more stable a-Si:H network is highly inhomogeneous containing highly ordered regions and regions with lower degree of order. The best hot wire a-Si:H samples contain only 1-3 at.% H with less SWE than GD a-Si:H which requires about 8 - 10 at.% H to optimize its properties. On the other hand, the creation and removal of light-induced defects of a-Si:H are closely linked to the hydrogen dynamics [8,9]. An understanding of H dynamics on a microscopic scale is essential for the understanding of light-induced metastability in a-Si:H.

One of the differences between the NMR study of hydrogen motion and that of hydrogen diffusion is that NMR detects both localized and delocalized motions. Furthermore, NMR is able to detect separately the motions associated with the isolated and the clustered hydrogen. Another advantage of NMR is its ability to probe atomic motions over a broad range of timescales. According to diffusion measurements[9], the jump rate leading to diffusion is very small even at elevated temperatures (less than 1 Hz). Since light-induced metastability occurs even at 2 K and can be recovered upon annealing below 200 K [10], diffusion of the majority of H atoms seems to be irrelevant at such low temperatures. Local H motions, which may not necessarily lead to long range diffusion, could be involved in the process of light-induced metastability. Deuterium NMR and dipolar order relaxation studies in GD a-Si:H [8,11] have provided some evidence for the existence of a significant amount of relatively mobile H (over 15% of the H content); H$_2$ molecules trapped in nanovoids have been suggested as the origin. We will present some further evidence indicating the existence of some mobile hydrogen; in this regard, it will be shown that significant differences exist between GD and hot wire a-Si:H films.

II.2 Experimental and Results of Dipolar Order Relaxation

Figire 5 shows the Jeener-Broekaert pulse sequence. Pulse width = 1 and 0.5 ms, (for H=9.4 T) τ = 5, 10, 100 ms are used. To explore the local motion for both clustered and isolated ^{1}H, we measure the echo height for a fixed τ, as a function of decay time t. The dipolar order relaxation times of the clustered and isolated ^{1}H are given in Figs. 6 and 7 for the GD and HW films.
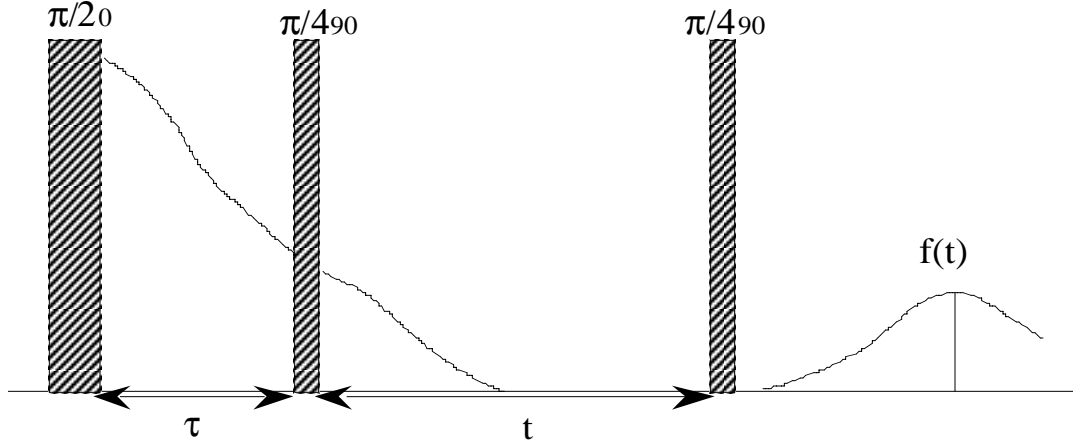
Fig.5 The Jeener-Broekaert pulse sequence.
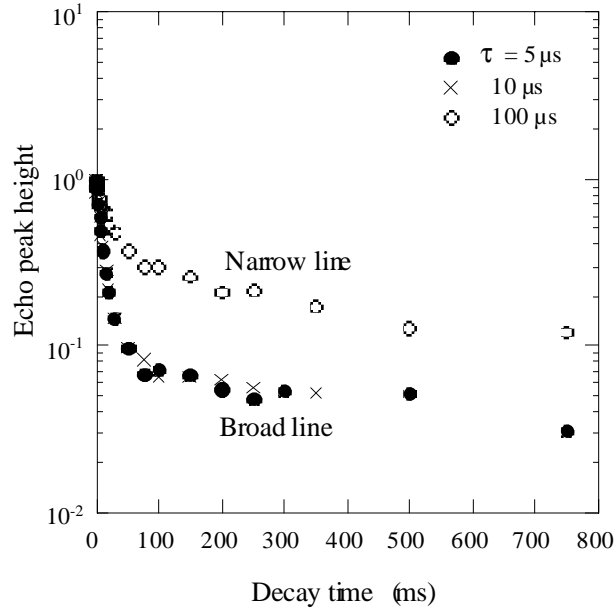
Fig.6 Dipolar order relaxation for a hot-wire film. τ = 5, 10 µs for broad line (clustered ^{1}H) τ = 100 µs for narrow line (isolated ^{1}H).
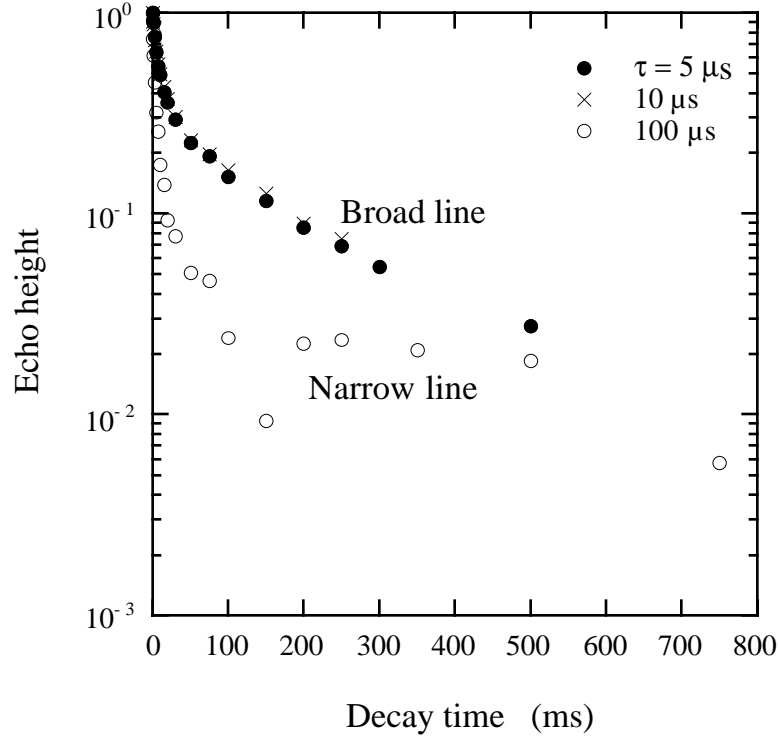
Fi.g.7 Dipolar order relaxation for a GD film for broad and narrow lines.

The results of the data fitting are given in Figs. 8-11. In Figs 9 and 11, one obtains the dipolar relaxation time T_{1D} by using a function $f(t) \propto \exp(-t/T_{1D})$ from the early decay data.
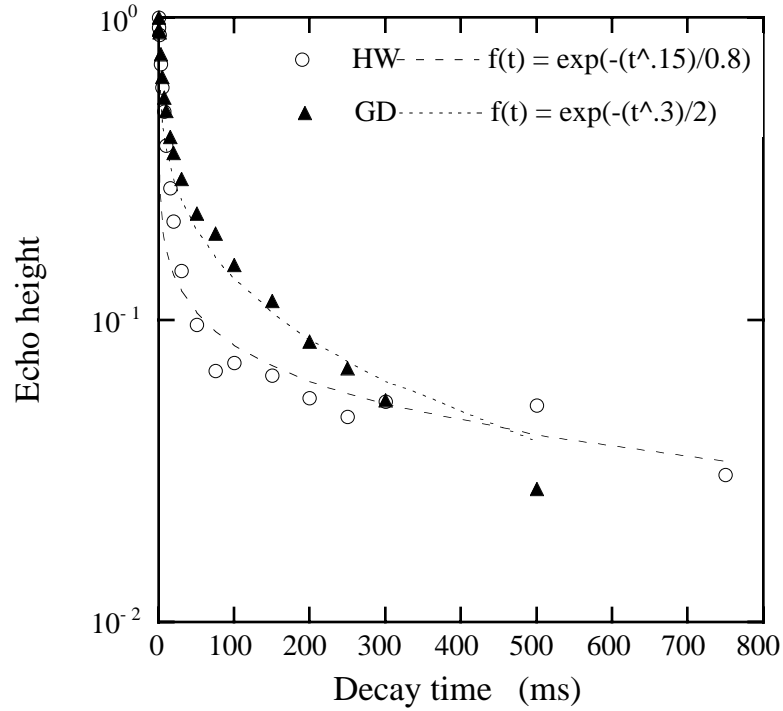
Fig.8 Compare dipolar order relaxation in HW and GD films.
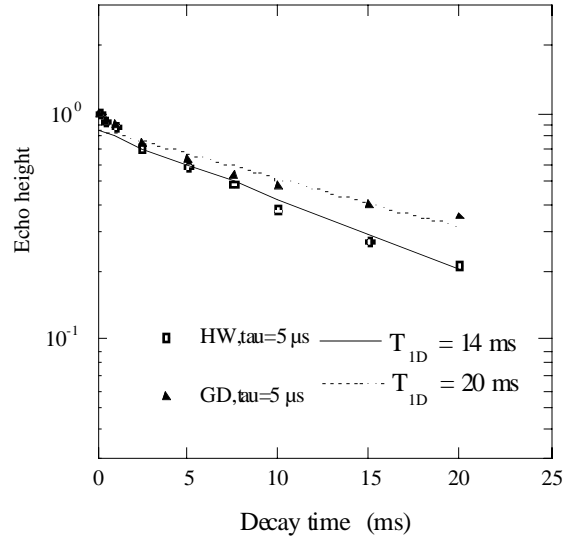
Fig. 9 Early decay of clustered ^{1}H (broad lines) can be fitted by $f(t) \propto \exp(-t/T_{1D})$ in both HW and GD a-Si:H.
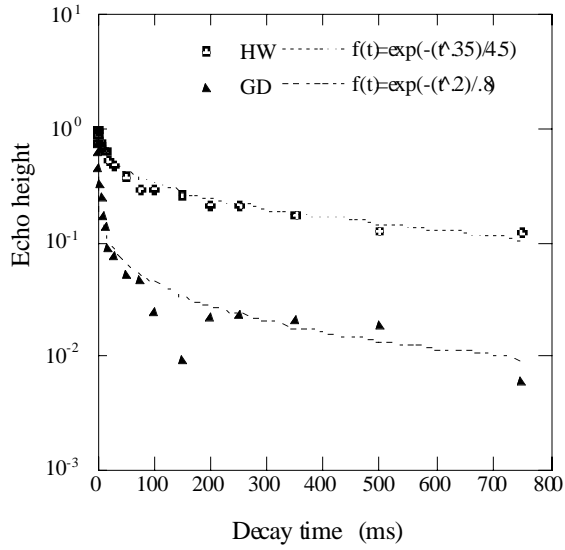
Fig. 10 Dipolar order relaxation of isolated ^{1}H, fitted by $f(t) = \exp(t^{\wedge X}/T_{1D})$ in GD and HW a-Si:H.
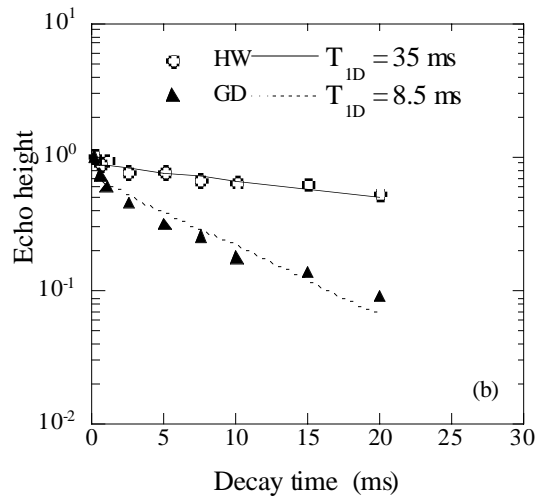
Fig. 11 Early decay of isolated ^{1}H (narrow lines) fitted by $f(t) \propto \exp(-t/T_{1D})$
in both HW and GD a-Si:H.

II.3 Summary of Dipolar Relaxation Data

From early dipolar relaxation time (< 20 ms) we deduced the T_{1D} by fitting the data to $f(t) \propto \exp(-t/T_{1D})$. At room temperature, the T_{1D} of the clustered H is slightly shorter but the T_{1D} of the isolated H is 4 times longer in HW film than that in GD films. The results may indicate that the local motion of the isolated H is much slower in HW compared to that in GD film. High temperature NMR studies are necessary to clarify the 1H motion.

Table III Dipolar relaxation time in the DG and HW films

T_{ID} / Sample	clustered ^{1}H (broad lines)	isolated ^{1}H (narrow lines)
GD	20 ms	8.5 ms
HW	14 ms	35.0 ms

II.4 High Temperature (room temperature to 200 °C) NMR

So far, no ^{1}H NMR study of hydrogen motion at temperatures above 60 °C has been reported. High temperature NMR is applied to investigate the hydrogen dynamics and microstructure of a-Si:H. A home-made high temperature NMR probe was used in the temperature range from room temperature to 200 °C. Preliminary results show an indication of hydrogen motion from room temperature to 150 °C (below 150 °C, the change of the proton spectrum with temperature is completely reversible; whereas, above 150 °C, the ^{1}H effusion occurs). In addition to the generic broad and narrow lines observed in all a-Si:H, a second narrow line (less than 1 kHz wide) is identified as the temperature is raised. This very narrow line is particularly visible and sensitive to temperature in hot-wire a-Si:H.

III. SWE AND THE STRESS OF HOT-WIRE A-SI:H

III.1 Introduction

Correlation between stress and SWE in a-Si:H have been studied by several groups.[12-14] Stutzmann [12] found that the number of metastable defects was proportional to the total stress in the film. On the other hand, Guha et al. [13] observed no correlation between photodegradation and stress; that is, the SWE was the same in both zero- and highly stressed films. The previous technique, however, was unable to measure the photo-induced change of the stress. Recently, using a newly developed technique with much higher sensitivity, a subtle increase of film stress was found in glow discharge (GD) a-Si:H films upon light soaking.[15] Their results indicated a photoinduced structure change with similar dynamics to the SWE. On the other hand, hot-wire (HW) a-Si:H with 2-3 at.% H has shown improved electronic stability. It is therefore interesting to study the film stress and its possible relation to the SWE behavior in the HW materials in comparison with the GD a-Si:H. We cooperated with Prof. S. Nitta's group at Gifu University, Japan and Qi Wang et al at NREL to complete a study of photo-induced stress and the SWE in hot-wire a-Si:H films, and presented a paper in the NCPV Program Review Meeting [16], concluding that there is no relationship between stress and light-induced degradation.

III.2 Samples and Experimental

1-μm thick a-Si:H films were deposited by HW CVD at substrate temperatures from 280 °C to 440 °C onto the following substrates: (a) crystalline silicon for IR absorption; (b) 2 mm $\times$ 20 mm $\times$ 100-μm-thick fused-quartz strip for stress, and (c) 7059 glass for conductivity measurements. Both the mechanical stress and the optoelectronic properties before and after light-soaking by a 300 mW/cm^2 white light were measured.

III.3 Results
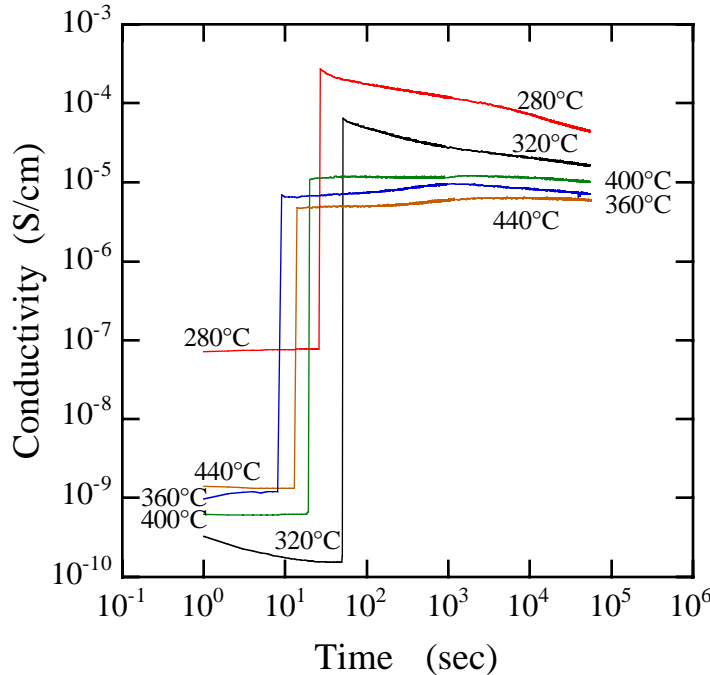
Fig. 12 Photoconductivities as a function of light-soaking time for the five hot-wire samples

We used the photoinduced changes in the photo-and dark- conductivities to study the SWE in hot-wire films. In Fig. 12 we show the conductivity values before and after illumination, and record the photoconductivity decay as a function of light-soaking time. We see that the photoconductivity decreases for the films deposited at T_s = 280 and 320 ˚C, but no obvious change occurs for the films deposited at $T_s \geq 360$ ˚C up to 15 h. by 300 mW/cm^2 light-soaking.

More information about the photo-induced electronic defect states can be obtained from the position of the Fermi level. To examine this, the temperature dependence of the dark conductivity was measured from room temperature up to 150 ˚C. We found that the activation energies changed from 0.60 to 0.83 eV, and from 0.82 to 0.9 eV upon light-soaking for the films deposited at the T_s of 280 ˚C and 320 ˚C, respectively. For the film deposited at 360 ˚C, the activation energy did not change. Small increases (from 0.76 to 0.79 eV and from 0.71 to 0.75 eV) were observed for the films deposited at 400 ˚C and 440 ˚C. Again, in agreement with the photoconductivity results, we found that the photo-degradation effect is very small in the hot-wire films deposited > 360 ˚C.

We have reported the initial stress of the a-Si:H films as a function of both the substrate temperature T_s and the total hydrogen content C_H. The maximum initial compressive stress ≈ 425 MPa corresponds to the lowest T_s = 280 ˚C and the highest C_H ≈ 8 at.%. As T_s increases, both C_H and the compressive stress decrease. The minimum compressive stress ≈ 74 MPa occurs at the highest deposition temperature (T_s = 440 ˚C) and the lowest C_H (< 1 at.%). In Fig. 13, we show the photo-induced changes of the stress by using the same 300 mW/cm^2 light-source.
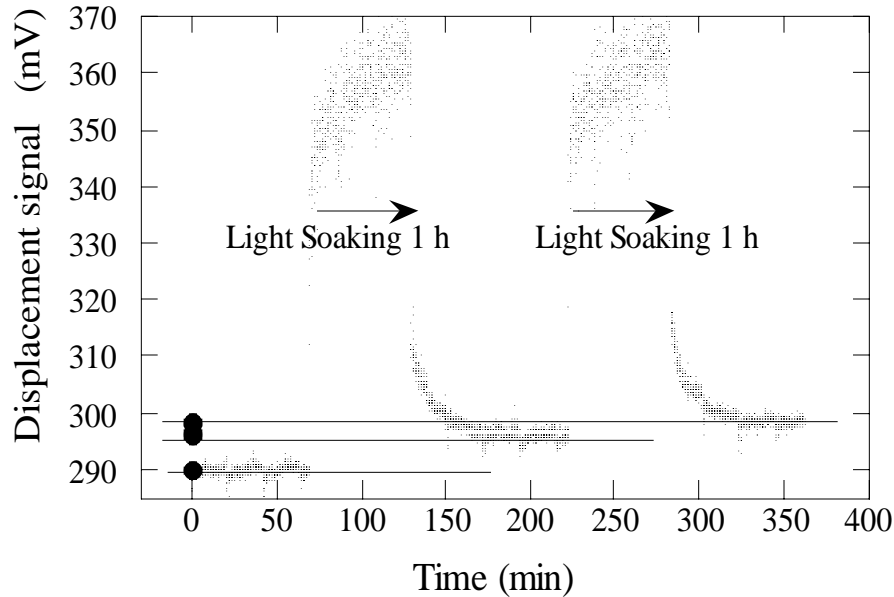
Fig. 13 Photo-induced changes of the stress in HW film deposited at 320 ˚C.

The low-case lines in Fig. 13 show the results of the photo-induced changes in the stress after first and second hour light soaking. The high signals during light-soaking result from temperature effect. The photo-induced changes can be recovered to their initial values by thermal annealing at 200 ˚C for 1 h.

We compare the above two kinds of photoinduced changes in the following. Fig. 14(a) shows that for all of these five hot-wire a-Si:H films, the photo-induced increase of the stress is on the order of 10^{-4} of the initial stress. The amount of the photo-induced change is the same as that

14

found in GD films.[15] In Fig. 14(b) we see the photoconductivity decrease in a factor of 4-6 for the films deposited at T_s = 280 and 320 °C, but there is negligible change for the films deposited at $T_s \geq 360$ °C. Therefore, the photo-induced volume expansion is not correlated to the SWE!
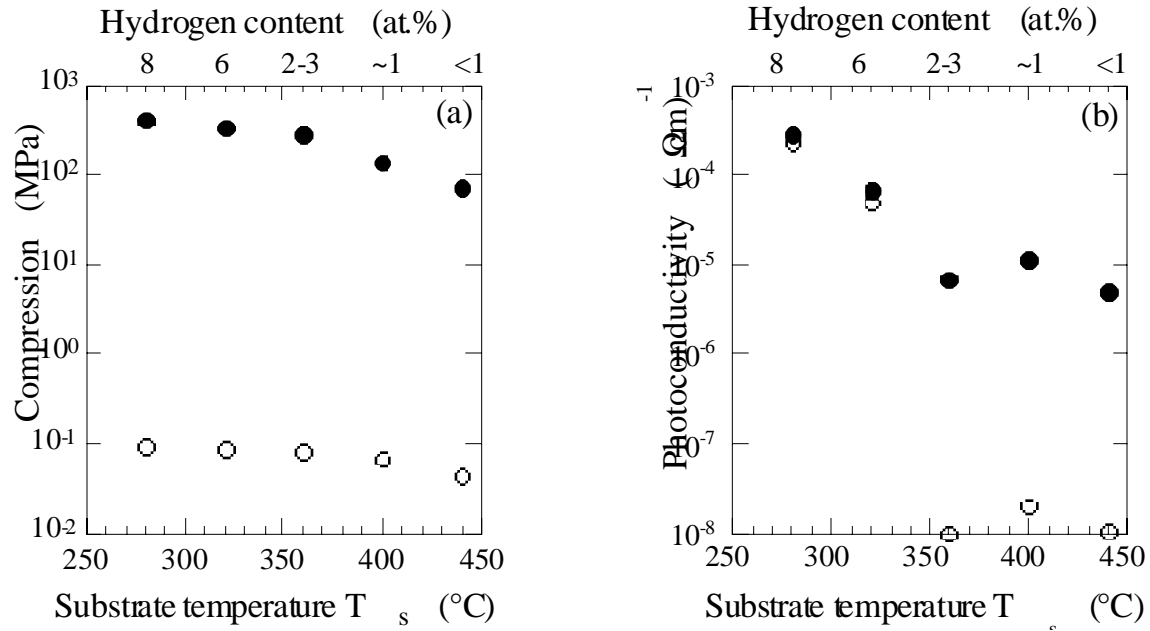
Fig. 14 The initial (●) and photoinduced changes (o) of (a) the compression, and (b) the photoconductivity for five hot-wire a-Si:H films deposited at varied temperature. Data in fig. 4(b) are from Fig. 3.

III.4 Sub-band Gap Absorption Measured by PDS and the Surface Morphology
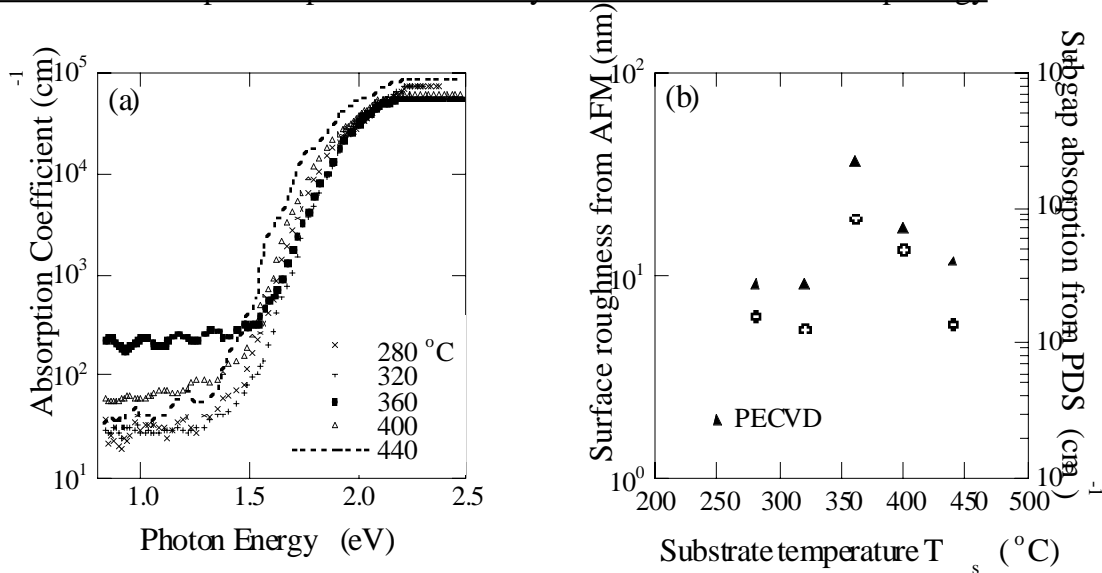
Fig. 15 (a) Sub-band gap absorption and the absorption edge measured by PDS, and (b) correlation of PDS (solid triangles) with AFM (open circuits) data shows the subgap absorption signal is due to surface roughness for the HW a-Si:H films. For reference, the sub-band gap absorption from a PECVD sample is also indicated.

Several techniques have been used to study the defect density of states and the absorption edge in a-Si:H films, such as the constant-photocurrent method (CPM), junction capacitance and transient photo-capacitance spectroscopy, and photo-thermal deflection spectroscopy (PDS). The CPM and capacitance results showed good agreement in that the density of defect states is $\leq$ 10^{16}/cm^3 for HW a-Si:H films with C_H in the range of 2-8 at. %. In Fig. 15(a) we present the first PDS results on HW a-Si:H films made at substrate temperatures from 280 to 440°C. We found that the sub-band gap absorption from PDS is one to two orders of magnitude higher than the CPM and capacitance results. Unexpectedly, the 360°C film shows the highest sub-band gap absorption which could correspond to a defect density $\geq 10^{18}$/cm^3 by using the relation $N_d =$ $7.9 \times 10^{15} \int \alpha_{ex}$ dE. Since we have had very reproducible results from the CPM method which have been calibrated using electron spin resonance (ESR), we know the defect density is $<$ 10^{16}/cm^3 for the film deposited at 360°C. A possible reason for this discrepancy could be the high sensitivity of the PDS technique to surface effects such as surface roughness, and that the absorption could be enhanced absorption in the bulk due to total internal reflection of the light at the rough surface.

Accordingly, we have examined the film surface morphology by AFM, and have plotted both the PDS and AFM results as a function of film deposition temperature in Fig. 15(b). The surface roughness was defined by an average in a scanning area of 1×1 μm^2, and was found to be in the range of 4-7 nm with an exception of two films deposited on 7059 glass for PDS measurements. The roughness of these films was found to be 18.98 nm and 13.44 nm for the 360 °C and 400 °C films, respectively. These are the films with the high PDS sub-band gap absorption. It is clear that there is a correlation between the PDS and the AFM data, and hence the sub-band gap absorption signal from PDS is due to surface roughness but not the bulk defect density for the HW a-Si:H films. As shown in Fig. 15(a), the PDS absorption signal increases exponentially with increasing photon energy, and the Urbach edge parameter E_u can be deduced. The value of E_u is the largest for the 360 °C film, but again, this value is affected by the surface roughness. We also comment that from the PDS data taken at the higher photon energies we were able to obtain the optical gap E_{opt} using a Tauc's plot. we found that $E_{opt} = 1.6 \pm 0.02$ eV for the film deposited around 360 °C.

III.5 Conclusions

It is clear that the less Si-H bonds the lower compression in the hot-wire films. We believe that this is also true in GD films. In GD films as T_s increases from 100 to 250 °C, the fraction of Si-H bond increases, and then the compression increases.

We observed a volume expansion and an increase of the IR absorption ~2000 cm^{-1} upon light soaking in all the a-Si:H films regardless of the preparation technique either by hot-wire or by H-diluted GD.[16-18] Biswas recent showed[19] a change in the oscillator strengths of Si-H vibrations due to the flipping of H to Si back-bond induced a 10^{-4}-10^{-3} increase in the 2000 cm^{-1} absorption. Meanwhile, the distortions of the structure could increase the strain of the network in the same order of magnitude. The question is: does the photoinduced volume expansion relate to the SWE? By measuring the PC vs. light-soaking time for the same group of hot-wire films, we show that these changes are not directly related. This is different from what has been observed in GD films[15]. In the HW films deposited at $T_s < 360$ °C, a factor of 4-6 photodegradation of the photoconductivity was obtained, but there was no obvious degradation of the photoconductivity for the films deposited at $360 < T_s < 440$ °C. It raises the questions of " in what condition the HW material is magic?" and how do we define the "magic material"?

More characterizations such as sub-band gap absorption are needed in addition to the PC measurements.

Finally, the surface roughness rather than the bulk defects were responsible for the high PDS signal in the hot-wire a-Si:H films.

IV. INTERNAL ELECTRIC FIELD PROFILE OF a-Si:H AND a-SiGe:H SOLAR CELLS

IV.1 Introduction

For high efficiency amorphous silicon solar cells, dual- or triple-junction tandem structures are used. The charge collection of the a-Si:H and a-SiGe:H cells are crucial for the short- and long wave length performance, respectively. Since the charge collection process in a-Si:H based solar cells depends upon field-assisted drift in the internal-electric-field, the knowledge of the electric-field profile is important for device design. One needs to know how the electric field distribution changes with i-layer thickness and the Ge content, and how this affects the V_{oc} and the quantum efficiency wavelength dependence. By using computer simulation, the relation of the electric field distribution with V_{oc} of a-Si based alloy p-i-n cells under steady state light illumination has been studied by Hack et al. [20] and Fonash et al. [21]. The results show that the electric field $E(x)$ decays exponentially from the junction interfaces. The value and the decay rates depend on the space charge density and the carrier's mobility. Assuming the internal field is screened by a constant midgap state, N_d, and neglecting the free carriers contribution, from the Poisson equation one obtains the field distribution from the junction interfaces decays exponentially. Here we consider the field decay from p/i interface as follows:

$$E_i(x) = E_0 e^{-\beta x} \tag{1}$$

where E_o is the field strength at the p/i junction interface, and x is the distance from the interface in the i layer. β is defined as $\beta = 1/L_o = \sqrt{qN_d/\varepsilon}$, where L_o is the screening length, the electron charge $q = 1.6 \times 10^{-19}$ coulomb, and the dielectric constant $\varepsilon = 10^{-12}$ F/cm. On the other hand, few experimental results have been published. Among them the transient-null-current method[22] is an attractive technique because the experimental knowledge of $E_i(x)$ can be obtained in a real p-i-n cell structure. We present the experimental results of $E_i(x)$ on a-Si:H and a-SiGe:H solar cells with varied i-layer thickness and Ge content by using the transient null-current method.

IV.2 Sample and Experiment

Samples were made at Energy Conversion Devices (ECD) by plasma-enhanced CVD. Several structures were studied i.e. a-Si:H stainless-steel/n-i-p/ITO cells with varied i-layer thickness, and a-SiGe:H ss/n-i-p/ITO cells with varied Ge content. The sample's parameters are listed in Tables I and II, respectively. A pulsed N_2 laser that pumped a dye laser in a wavelength range of 380-640 nm was used for the photo excitation. Neutral density filters were used to adjust the incident light flux. The pulse light was illuminated through the semi-transparent ITO and wide-band gap p-layer on to the intrinsic layer. A 150 MHz pulse generator with 1×10^{-11} sec resolution was used to apply a positive voltage pulse V_a. The measurements were made at room temperature. The detailed experimental conditions can be found elsewhere. [23,24]

<u>IV.3 Results</u>

IV.3.1 Dependence of the Electric Field Profile on i-layer Thickness

Figure 16(a) shows the applied voltage $V_a(\lambda)$ as a function of the laser wavelength λ for the a-Si:H cells with varied i-layer thickness. The dashed lines are the fitting curves according to Eq. (1) by using the $E_i(x)$ functions shown in Fig. 16(b). $E_i(x)$ is only shown near the p/i interface since that is where it is most valid. One can see that V_a decreases drastically when $\lambda > 475$ nm in 0.1 and 0.2-μm-thin cells. We believe this is due to the hole transport evolving when the photo-excited carriers were generated through the thin i-layer as discussed below. V_a decreases smoothly in 0.4 and 0.5-μm-thick cells. The best-fit parameters are listed in Table I. The values of N_d in thin cells can not be simply deduced from $\beta=1/L_o=\sqrt{qN_d/\varepsilon}$ in thin cells, because of the strong influence on $E_i(x)$ from the n/i junction.

Table IV ss/n-i-p/TCO solar cell performance and the fitting parameters of $E_i(x)$

Sample ID	i-layer thickness (μm)	V_{oc} (V)	J_{sc} (mA/cm^2)	FF	P_{max} (mW/cm^2)	E_o (V/cm)	β (μm)$^{-1}$	L_o (μm)	N_d (cm^{3}eV)$^{-1}$
LL843	0.1	0.945	8.67	0.70	5.73	1.15×10^5	1.12	0.89	–
LL794	0.2	0.949	11.29	0.66	7.05	5.32×10^4	2.57	0.37	–
LL795	0.4	0.947	13.23	0.57	7.11	2.7×10^4	8.00	0.13	4×10^{16}
LL793	0.5	0.947	13.25	0.55	6.93	2.0×10^4	7.00	0.14	3×10^{16}
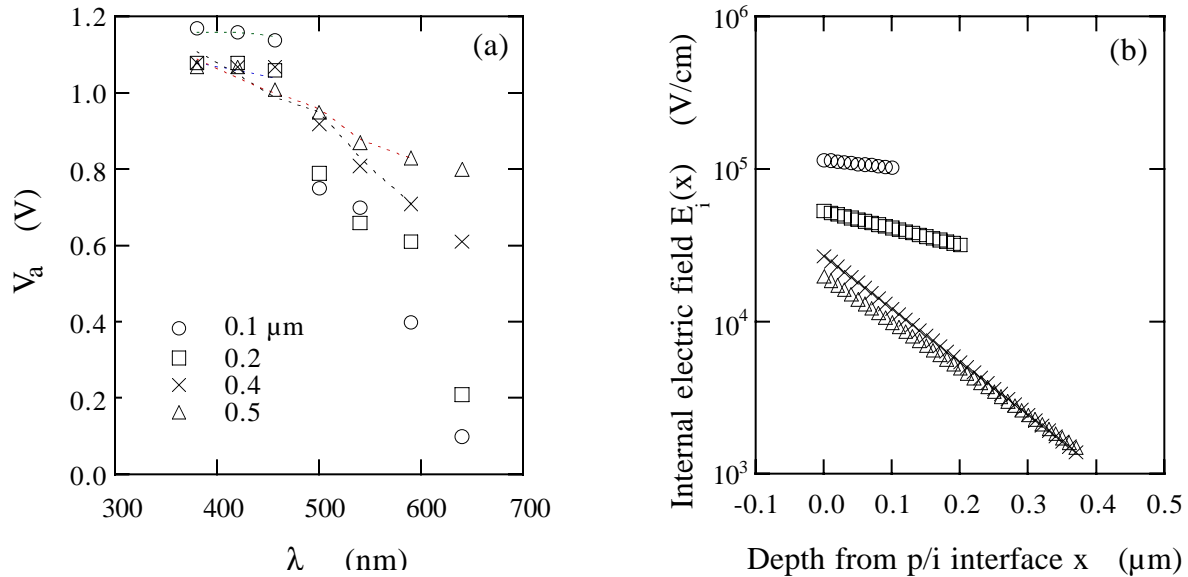
Fig. 16 (a) Applied voltage V_a vs. the laser wavelength λ in the a-Si cells, and
(b) the $E_i(x)$ functions used for the best fit, shown by the dotted lines in (a).

In Figure 17(a), we plot the cell performance as a function of the i-layer thickness. One can see that V_{oc} almost does not depend on the i-layer thickness L, but the short-circuit current J_{sc} increases with increasing L. The overall performance P_{max} increases first and then is saturated

18

when $L = 0.2$ μm, because the combination of the increasing of J_{sc} and the decreasing of the fill factor FF. Figure 17(b) shows the internal electric field parameters as a function of the i-layer thickness L. Both E_O and L_O decrease with increasing L. Interestingly, V_{oc} does not depend on the internal field distribution, no matter how much the internal field distribution (E_O and L_O) changes with the i-layer thickness.
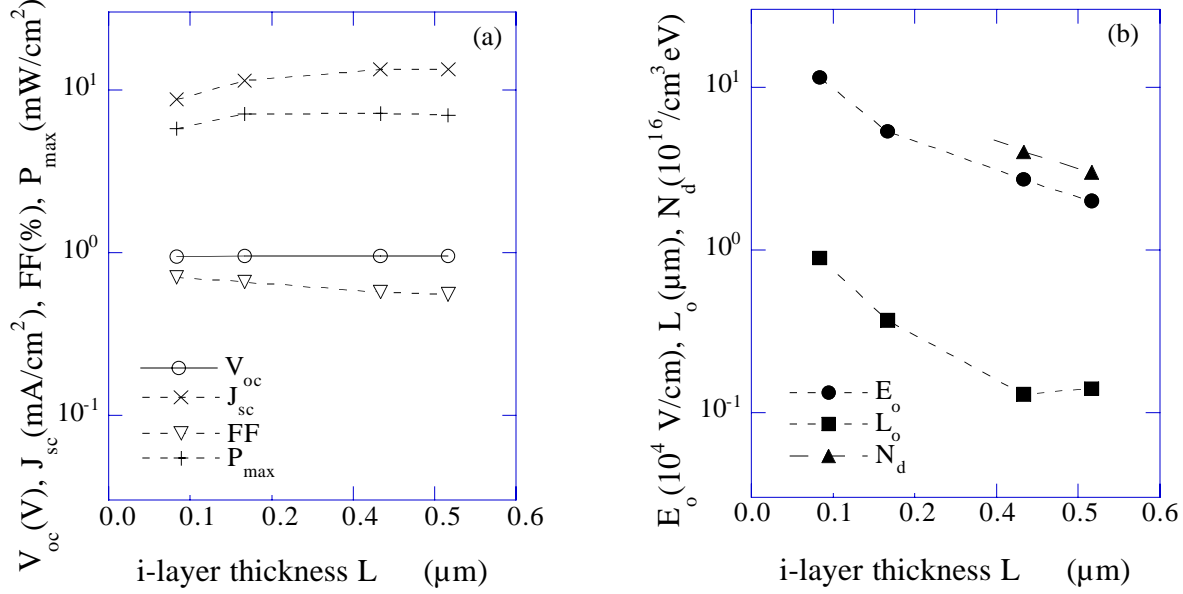
Fig. 17 (a) the a-Si cell performance and (b) the internal field parameters as a function of the i-layer thickness.

IV.3.2. The electric field profile of a-SiGe:H solar cells with varied Ge content
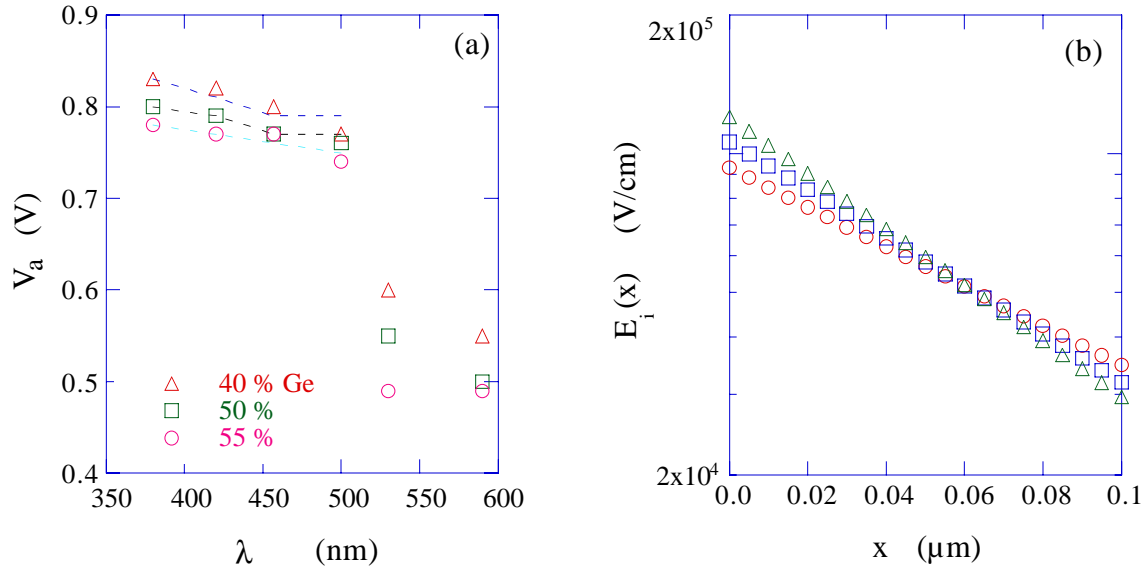
Fig. 18 (a) V_a vs. λ for the 0.15 μm a-SiGe cells with varied Ge content. The dotted lines are the fits to the data by using the $E_i(x)$ functions in (b).

19

An increased Ge ratio will reduce the band gap of a-SiGe:H materials. We studied the electric field profile of 0.15-µm-thin a-SiGe:H ss/n-i-p/TCO cells with different Ge contents. Figure 18(a) plots the measured V_a vs. λ. One can see again that V_a decreases quickly when $\lambda > 500$ nm in the 0.15-µm-thin cells. We simulated the data for wavelengths less than 500 nm by using the functions in Fig. 18(b). The fits to the data are shown in Fig. 18(a) as the dashed lines. The cell performance, the fitting parameters of $E_i(x)$ and the deduced defect density N_d are listed in Table II. We can see that the electric field is stronger for the cell with less Ge content. This is because of a larger optical gap and less defects in the a-SiGe:H i-layer with less Ge content. [8]

Table V. ss/n-i-p/TCO solar cell performance and the fitting parameters of $E_i(x)$

Sample ID	Ge:Si	V_{oc} (V)	J_{sc} (mA/cm^2)	FF	P_{max}	E_o (V/cm)	β (µm)$^{-1}$	L_o (µm)	N_d (cm^{3}eV)$^{-1}$
L1	55:45	0.574	14.83	0.540	4.60	9.31×10^4	9.886	0.10	9.7×10^{16}
L2	50:50	0.673	13.60	0.556	5.09	1.06×10^5	12.02	0.083	1.4×10^{17}
L3	40:60	0.700	12.01	0.630	5.33	1.20×10^5	14.01	0.071	2.0×10^{17}
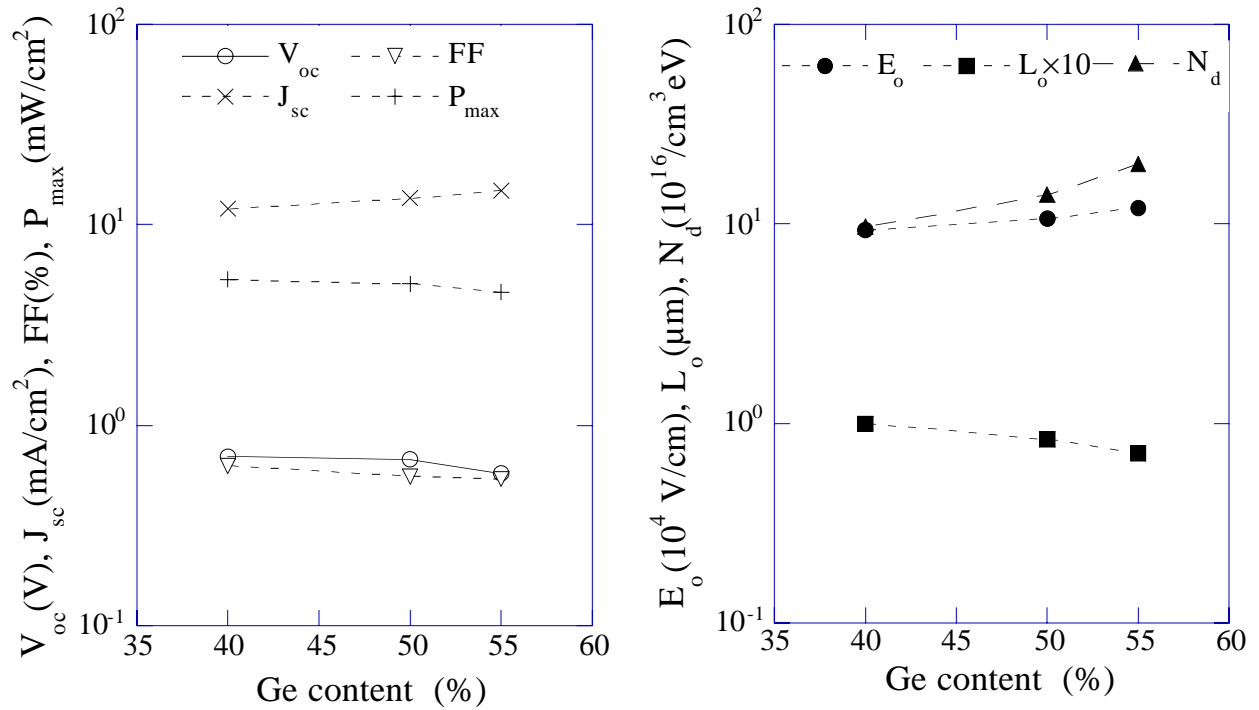
Fig. 19 (a) The cell performance and (b) the internal field parameters as a function of the Ge content in the a-Si-Ge i-layer.

Figure 19(a) shows the cell performance as a function of the Ge content in the a-Si-Ge:H layer. One can see that V_{oc}, FF and P_{max} decrease but J_{sc} increases with increasing Ge content. Figure 19(b) shows the internal field parameters E_o, L_o and N_d as a function of the Ge content. Although the values for L_o and N_d displayed in figure 19(b) are slightly different for different samples, they are the same within the uncertainty of the fitting technique - one should consider the N_d values only as an order of magnitude estimate of the defect density. That is because we were only able to use four data points in the fit for each sample, excluding the long-wavelength data as discussed below.

IV.4 Summary and Discussions

We have studied two groups of solar cells: (a) a-Si:H p-i-n solar cells with varied i-layer thicknesses, and (b) a-SiGe:H cells with varied Ge content. When using an exponential function $E_i(x)=E_0 e^{-\beta x}$ to fit the experimental results, we obtained the field strength at the p/i interface E_0, the screening length L_0, and the density of defect states N_d in the i-layer. From the group (a) samples, our results indicate that for the same quality materials, the thinner the i-layer, the stronger the electric field strength obtained. Whereas V_{oc} does not change with the i-layer thickness, the internal field profile changes. Both theoretical and experimental studies of the open-circuit voltage, V_{oc}, of a-Si solar cells have found that the value of V_{oc} not only depends on the Fermi-level difference of the n- and p-layers, but also on the quality of the p/i interface as well as the i-layer. Especially, V_{oc} in some devices is dominated by carrier recombination at the p/i junction. The demonstration of an independent value of V_{oc} on the field profile implies high-quality p/i interfaces in this group of cells. And then both the built-in potential E_{bi} and the V_{oc} depend on the Fermi-level difference of the n- and p-layers. An increase in the i-layer thickness results in an increase of J_{sc} but a decrease of FF. The latter is due to the thicker the i-layer the lower the field strength, consequently the less charge collection. Since the critical electric field strength is $\xi_c = kT/qL_p$, for the minority carrier diffusion length $L_p \approx 0.25$ µm, ξ_c is of the order of 10^3 V/cm.[20] As shown in Fig. 18(b), $E_i(x) > 10^3$ V/cm when L < 4000 Å which is in agreement with the device design for high performance solar cells. For the group (b) a-SiGe:H cells, the electric field is stronger for the cell with less Ge content. This is because of a larger optical gap in the a-SiGe:H i-layer with less Ge content. One can compare the experimental results of the internal electric field profile with the cell performance as shown in figs. (2) and (4), and then deduce useful information for the device design.

One notices a drastic decrease of V_a when $\lambda > 500$ nm as shown in Figs. 16(a) and 18(a) in 0.1 - 0.2 µm thin cells. We tend to explain qualitatively the effect of hole limitation as follows. The applied voltage, V_a, is proportional to the peak value of the transient photocurrent j_{pc} which corresponds to the collected photocarrier density per second by the internal field $E_i(x)$. The photogenerated holes will drift toward the p-side, and the electrons toward the n-side in the internal electric field $E_i(x)$. When the short wavelength light illuminates from the p-side, the e-h pairs are generated near the p/i interface due to the shallow absorption depth. The holes will be swiped out through the thin p-layer quickly and the electrons drift oppositely through the i-layer. Since the electron mobility is ten times larger than the hole's, they quickly move through the i-layer. As the wavelength increases, the e-h pairs are generated through the i-layer and then the hole-limitation effect becomes more and more important. When e-h pairs are generated near the n/i interface, the holes must travel through the i-layer with a low mobility that becomes the limitation factor for the photocurrent j_{pc}. However, the above argument can not explain why the 0.1-0.2 µm-thin cells exhibit a decrease of V_a at shorter wavelengths as shown in Fig. 16(a). There must be an interface-related reason such as trapped holes near the n/i interface that result in a barrier which depresses the carrier transport.

V. EL AND PL SPECTRA IN A-SI:H

Based on the systematical studies of the efficiency, the temperature dependence, and the energy spectrum of electroluminescence (EL) in a-Si:H p-i-n cells, we have developed a complete model to explain the EL features as dispersive-transport-controlled non-geminate recombination processes. The results were given in the last final report.[23] However, most of the EL spectra were taken by the home-made filter wheels and few of them were taken by a grating monochromater in other labs. There were only 12-14 data points of a spectrum in the energy range of 0.6 eV to 1.6 eV, and the filter bandwidth was 80-90 nm. The resolution of the spectra

was very poor as shown in Fig. 20(a). Therefore, we were looking forward to using a grating spectrometer to study the spectral lineshape in more detail.

During the last 4 months we have successfully upgraded our EL systems by installing a grating spectrometer (SPEX TRIAX-180) and the LabVIEW software. As shown in Fig. 20(b) we now obtain EL spectra not only more precisely but also more efficiently. We have measured EL spectra from a group of a-SiGe:H cells from U. Toledo. Meanwhile, we use the same system for PL measurements. We have measured excitation wavelength dependence of PL from a group of films deposited on varied substrate conditions at United Solar. Both the EL- and PL- data analysis are being undertaken.
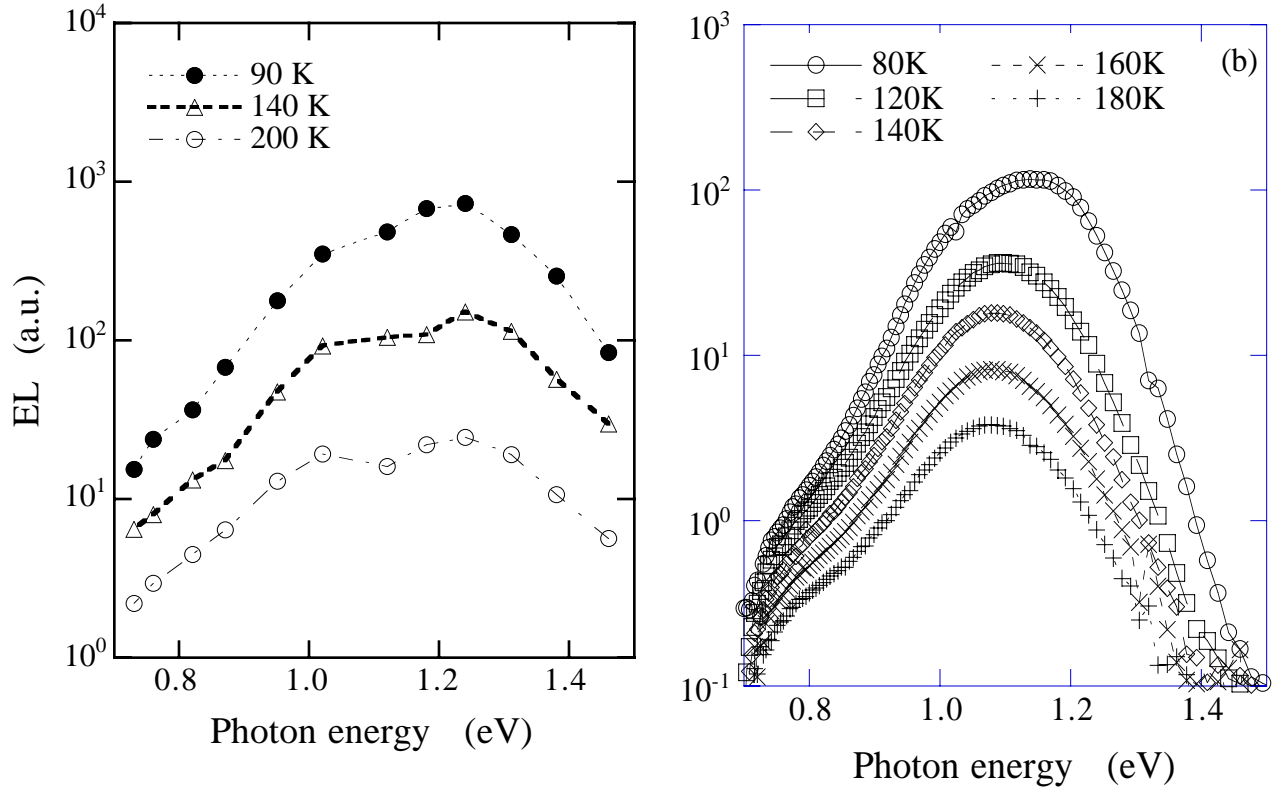
Fig. 20 (a) The EL spectra taken by the filter spectrometer from a 0.5 μm a-Si:H p-i-n cell made at Solarex.

(b) The EL spectra taken by the grating spectrometer from an a-Si:H p-i-n cell made at Solarex.

FURTHER RESEARCH

(1) Establish the feasibility to detect hydrogen motion in a-Si:H by measuring NMR spectra above room temperature.

(2) Complete a detailed characterization of H-motion, -bonding, and light-induced changes in hot-wire material in comparison to glow discharge material.

(3) Study the substrate and the deposition condition effects on the optoelectronic properties of a-Si:H based film by PL, EL and $E_i(x)$ for GD and hot-wire CVD samples.

(4) Study The transport properties in films from a-Si:H to μc-Si:H.

(5) Study the questions of " in what conditions the hot-wire materials are magic?" and how to we define the "magic material"? by characterizing the PC, the sub-band gap absorption, and the position of Fermi level before and after light-soaking in several groups of hot-wire films.

Publications:

1. Temperature dependence of the optical absorption edge in C_{60} thin films, Tamihiro Gotoh, Shuichi Nonomura, Hideki Watanabe, Shoji Nitta, and Daxing Han, Phys. Rev. B**58**, 10060 (1998).
2. Temperature dependence of conductivity and the effect of oxygen intercalation in C_{70} film, Daxing Han, Hitoe Habuchi, and Shoji Nitta, Phys. Rev.B **57**, 3773 (1998).
3. Correlation of stress with hydrogen micro-structure in Thin Film Hydrogenated Amorphous Silicon, Daxing Han, T. Gotoh, Motoi Nishio, S. Nonomura, S. Nitta, Qi, Wang, E. Iwaniczko. MRS Symp. Proc. Vol **505** (Material Research Society, 1998), p.445.
4. Internal Electric Field Profile of a-SiGe p-i-n Solar Cells, Xinhua Geng, Xunming Deng, Qi Wang, and Daxing Han, to be published in MRS-98 proc.
5. Light-induced change of Si-H bond absorption in Hydrogenated Amorphous Silicon, Guozhen Yue, Jonathan Baugh, Liangfan Chen, Qi Wang, Eugene Iwaniczko, Guanglin Kong, Yue Wu, Daxing Han, to be published in MRS-98 proc.
6. Photo-induced Structure Metastability and the SWE in a-Si:H, Daxing Han, Tamihiro Gotoh, Motoi Nishio, Tomonari Sakamoto, Shuichi Nonomura, Shoji Nitta, Qi Wang, Eugene Iwaniczko, Harv Mahan, to be published in NCPV Program Revive Meeting (Sept., 1998).

References:

1. H. M. Branz, *Solid State Communications,* **105/6**, 387 (1988).; MRS Spring Meeting Proc. Symp. A, 1998, in press.
2. R. Arya, Final Technical Report (13 Sept. 94-28 Feb. 98), NREL/SR-520-24854, June 1998.
3. D.E. Carlson, R.W. Smith, P.J. Zanzucchi, and W.R. Frenchu, in *Pro. IEEE Photovoltaics Specialists Conf.*, 16th, (SanDiego, CA, pp. 1372-1375. IEEE, New York, 1982).
4. R. Darwich et al., *Philosophical Magazine* B, **72**, 363-372 (1995).
5. Yiping Zhao, Guaglin Kong, Guanggin Pan, and Xianbo Liao. *Phys. Rev. Lett.* **74**, 558 (1995); G. L. Kong, D. L. Zhang, Y. P. Zhao, G. S. Sun, G. Q. Pan, and X. B. Liao, *J. Non-Cryst. Solids* **164/166**, 211 (1993);Solid State Phenomena, **44/46**, Part 2: p677-684 (1995).
6. J.D. Holbech, B. Bech Nielsen, R. Jones, P. Sitch, S. Oberg, *Phys. Rev. lett.* **71**, 875 (1993).
7. Y. Wu, Y., J. T. Stephen, D. X. Han, J. M. Rutland, R.S. Crandall, and A. H. Mahan, Phys. Rev. Lett. **77**, 2049 (1996).
8. P. Hari, P. C. Taylor, and R. A. Street, Mater. Res. Soc. Proc. **336**, 329 (1994).
9. H. M. Branz, S. E. Asher, and B. P. Nelson, Phys. Rev. **B47**, 7061 (1993).
10. Daxing Han, M. Yoshida, and K. Morigaki, J. Non-Cryst. Sol. **97/98**, 651 (1987).
11. R. E. Norberg, P. A. Fedders, and D. J. Leopold Mater. Res. Soc. Symp. Proc. **420**, 475 (1996).
12. M. Stutzmann, *Appl. Phys. Lett.* **47**, 21 (1985).
13. S. Guha, W. den Boer, S.C. Agarwal, and M. Hack, *Appl. Phys. Lett.* **47**, 947 (1985).
14. S. R. Kurth, Y. S. Tsuo, and R. Tsu, *Appl. Phys. Lett.* **49**, 951 (1986).
15. T. Gotoh, S. Nonomura, M. Nishio, N. Masui and S. Nitta, Proc of 17th International Conference on Amorphous and Microcrystalline Silicon, in *J. Non-Cryst. Sol* (1998).
16. Daxing Han, Tamihiro Gotoh, Motoi Nishio, Tomonari Sakamoto, Shuichi Nonomura, Shoji Nitta, Qi Wang, Eugene Iwaniczko, Harv Mahan, to be published in NCPV Program Revive Meeting (Sept., 1998).
17. Daxing Han, T. Gotoh, Motoi Nishio, S. Nonomura, S. Nitta, Qi, Wang, E. Iwaniczko. MRS Symp. Proc. Vol **505** (Material Research Society, 1998), p.445.
18. Guozhen Yue, Jonathan Baugh, Liangfan Chen, Qi Wang, Eugene Iwaniczko, Guanglin Kong, Yue Wu, Daxing Han, to be published in MRS-98 proc.
19. R. Biswas, 10 th NREL-EPRI a-Si team meeting, (Aug. 1998, Copper Mountain, CO).
20. M. Hack and M. Shur, J. Appl. Phys. **58**, 997 and 1656 (1985); **55**, 4413 (1984).
21. J.K. Arch, F.A. Rubinelli, J.-Y. Hou, and S. J. Fonash, J. Appl. Phys., **69**, 7057 (1991).
22. T. Datta and M. Silver, Appl. Phys. Lett. **38**, 903 (1981).
23. Daxing Han, Final Subcontract Report (July 7, 94-Jan.15, 98), NREL/SR-520-24741, May. 1998.
24. Internal Electric Field Profile of a-SiGe p-i-n Solar Cells, Xinhua Geng, Xunming Deng, Qi Wang, and Daxing Han, to be published in MRS-98 proc.

Abstract

This report describes studies on GD and hot-wire a-Si based samples by UNC-CH during Phase I. We have characterized H-bonding and its light-induced changes by using IR and DIR. For the less stable film, there is a simultaneous decrease ~ 2040 cm^{-1} and increase ~ 1880 cm^{-1}; for the more-stable samples, the DIR near 2000 cm^{-1} increases upon light soaking. NMR dipolar relaxation time T_{1D} of the clustered H is slightly shorter but the T_{1D} of the isolated H is 4 times longer in HW film than that in GD films. The results indicate that the local motion of the isolated H is much slower in HW compared to that in GD film. High temperature NMR results show a second narrow line (less than 1 kHz wide) as the temperature is raised. In stress measurements, it is clearly shown that hot-wire films with lower hydrogen content show lower compression . A photoinduced increase of the compression on the order of 10^{-4} of the initial value upon light-soaking was found in all the a-Si:H films whereas the Steabler Wronski degradation was similar. Hence the volume expansion is not directly related to SWE. Besides, we have measured the field profile in a-Si:H and a-SiGe:H solar cells, the results were in agreement with computer simulation.

REPORT DOCUMENTATION PAGE

Public reporting burden for this collection of information is estimated to average 1 hour per response, including the time for reviewing instructions, searching existing data sources, gathering and maintaining the data needed, and completing and reviewing the collection of information. Send comments regarding this burden estimate or any other aspect of this collection of information, including suggestions for reducing this burden, to Washington Headquarters Services, Directorate for Information Operations and Reports, 1215 Jefferson Davis Highway, Suite 1204, Arlington, VA 22202-4302, and to the Office of Management and Budget, Paperwork Reduction Project (0704-0188), Washington, DC 20503.

1. AGENCY USE ONLY (Leave blank)	2. REPORT DATE April 1999	3. REPORT TYPE AND DATES COVERED Annual Technical Progress Report, 16 January 1998–15 January 1999

4. TITLE AND SUBTITLE Search for Factors Determining the Photodegradation in High-Efficiency a-Si:H-Based Solar Cells; Annual Technical Progress Report, 16 January 1998–15 January 1999	5. FUNDING NUMBERS C: XAK-8-17619-11 TA: PV905001
6. AUTHOR(S) D. Han	

7. PERFORMING ORGANIZATION NAME(S) AND ADDRESS(ES) Department of Physics University of North Carolina Chapel Hill, NC 27599-3255	8. PERFORMING ORGANIZATION REPORT NUMBER

9. SPONSORING/MONITORING AGENCY NAME(S) AND ADDRESS(ES) National Renewable Energy Laboratory 1617 Cole Blvd. Golden, CO 80401-3393	10. SPONSORING/MONITORING AGENCY REPORT NUMBER SR-520-26522

11. SUPPLEMENTARY NOTES

NREL Technical Monitor: B. von Roedern

12a. DISTRIBUTION/AVAILABILITY STATEMENT National Technical Information Service U.S. Department of Commerce 5285 Port Royal Road Springfield, VA 22161	12b. DISTRIBUTION CODE

13. ABSTRACT *(Maximum 200 words)*

This report describes studies on glow discharge (GD) and hot-wire a-Si-based samples by the University of North Carolina-Chapel Hill during Phase I. We have characterized H-bonding and its light-induced changes by using infrared (IR) and differential IR (DIR). For the less stable film, there is a simultaneous decrease ~ 2040 cm^{-1} and increase ~ 1880 cm^{-1}; for the more-stable samples, the DIR near 2000 cm^{-1} increases upon light-soaking. Nuclear magnetic resonance (NMR) dipolar relaxation time T_{1D} of the clustered H is slightly shorter, but the T_{1D} of the isolated H is 4 times longer in hot-wire (HW) film than that in GD films. The results indicate that the local motion of the isolated H is much slower in HW compared to that in GD film. High-Temperature NMR results show a second narrow line (less than 1 kHz wide) as the temperature is raised. In stress measurements, it is clearly shown that HW films with lower hydrogen content show lower compression. A photoinduced increase of the compression on the order of 10^{-4} of the initial value upon light-soaking was found to be similar in all a-Si:H films which exhibit different amounts of Staebler-Wronski (SW) degradation. Hence, the volume expansion is not directly related to SW effect. Also, we have measured the electric field profile in a-Si:H and a-SiGe:H solar cells, and the results agreed with computer simulation.

14. SUBJECT TERMS photovoltaics ; photodegradation ; high-efficiency cells ; amorphous silicon films	15. NUMBER OF PAGES 34
	16. PRICE CODE

17. SECURITY CLASSIFICATION OF REPORT Unclassified	18. SECURITY CLASSIFICATION OF THIS PAGE Unclassified	19. SECURITY CLASSIFICATION OF ABSTRACT Unclassified	20. LIMITATION OF ABSTRACT UL